Nuclear Instruments and Methods in Physics Research A 610 (2009) 188–191

Contents lists available at ScienceDirect

Nuclear Instruments and Methods in Physics Research A

journal homepage: www.elsevier.com/locate/nima

Optimizing the timing resolution of SiPM sensors for use in TOF-PET detectors

R. Vinke [a,*], H. Löhner [a], D.R. Schaart [b], H.T. van Dam [b], S. Seifert [b], F.J. Beekman [b], P. Dendooven [a]

[a] Kernfysisch Versneller Instituut, University of Groningen, Zernikelaan 25, 9747 AA Groningen, The Netherlands
[b] Delft University of Technology, Mekelweg 15, 2629 JB Delft, The Netherlands

ARTICLE INFO

Available online 27 May 2009

Keywords:
Positron emission tomography
Silicon photomultiplier
Timing resolution
TOF-PET

ABSTRACT

We have investigated the timing performance of Hamamatsu Multi-Pixel Photon Counter (MPPC) photosensors in light of their use in time-of-flight (TOF) positron emission tomography detectors. Measurements using picosecond laser pulses show a single photo-electron root-mean-square (RMS) timing resolution down to about 100 ps. In coincidences of 511 keV photons detected with an LYSO crystal coupled to a MPPC and a BaF_2 detector, an optimum FWHM timing resolution of 600 ps was obtained with leading edge time pickoff at the 1–1.5 photo-electron level. By optimizing the LYSO/MPPC coupling, this can be improved by a factor of 2. We further conclude that the use of stored digitized pulses allows great flexibility and efficiency in developing data analysis algorithms.

1. Introduction

In time-of-flight positron emission tomography (TOF-PET), the time difference in the detection of two 511 keV annihilation photons is used to narrow down the position of positron annihilation on the line-of-response between two detectors. Improving on spatial resolution of present-day whole-body PET scanners (about 3–5 mm) would require a timing resolution better than ~30 ps. Present technology is far from reaching this goal; the only commercially available TOF-PET scanner has a timing resolution of ~600 ps [1]. In the foreseeable future the great advantage of TOF-PET is in reducing the image noise rather than allowing a direct determination of the annihilation position [2].

Several TOF-PET scanners using BaF_2 and CsF scintillator detectors were developed in the 1980s [3]. These efforts were abandoned with the advent of the BGO scintillator, due to its higher detection efficiency. The more recent discovery of scintillators such as L(Y)SO (highly efficient and fast) and $LaBr_3$ (very bright and fast) has revived the TOF-PET research and it is to be expected that many PET scanners will soon be TOF-capable.

In parallel with advances in scintillator materials, new fast and cost-effective photosensors are being developed. The so-called silicon photomultiplier (SiPM) is at the forefront of this development [4]. It combines low noise, high gain and fast timing. Single photo-electron timing resolutions close to 50 ps root-mean-square (RMS) have been reported [5]. SiPMs are insensitive to high magnetic fields, making them compatible with a Magnetic Resonance Imaging (MRI) environment and thus suitable for combined PET/MRI scanners (e.g. Ref. [6]).

We are developing novel PET detector technology based on monolithic scintillators and pixellated light sensors [7]. This concept promises improved sensitivity and spatial resolution. We are giving high priority to TOF capability and compatibility with an MRI environment, two of the major technological focus points in PET technology today. To meet these requirements, we use SiPM light sensor arrays.

The aim of the present work is to improve the timing capabilities of SiPM-based scintillation detectors through the development of optimized fast amplifiers and time pickoff techniques.

2. Experimental set-up

In all measurements described here, signal traces were digitized using an Acqiris DC282 digitizer with 10 bit resolution and, when using one input channel, an 8 GS/s sampling rate. Data presented here were obtained using two input channels, resulting in 4 GS/s for each channel. The advantage of this approach in which the full detector signals are stored is that analysis algorithms can be developed and optimized using the same data set. This allows great flexibility and removes any suspicion of changing experimental conditions that might arise in extensive measurement series.

The basic timing properties of SiPMs from Hamamatsu (the so-called Multi-Pixel Photon Counter, MPPC) were investigated using a picosecond laser. A Hamamatsu PLP10-40 laser

* Corresponding author.
E-mail address: vinke@kvi.nl (R. Vinke).

0168-9002/$ - see front matter © 2009 Elsevier B.V. All rights reserved.
doi:10.1016/j.nima.2009.05.068

diode head (wavelength 405 nm) with C10196 Controller was used. The laser pulse width is ~70 ps; time jitter with the "synch out" output from the Controller is less than 10 ps; 1 mm^2 MPPCs with microcell sizes 25×25, 50×50 and $100\times100\,\mu m^2$ (models S10362-11-025U, -050U and -100U), thus having, respectively, 1600, 400 and 100 microcells, were illuminated with laser pulses with intensity regulated using neutral density filters. The MPPC signals were amplified by a custom-built fast voltage amplifier (amplification factor 10), giving an average signal rise time of 1.2 ns. The amplifier output and the laser controller synch out were sent to the Acqiris digitizer and events containing both digitized traces were stored.

In a second set of measurements, a $2\times2\times8$ mm^3 LYSO crystal was mounted on the MPPCs. Using a ^{22}Na source, coincidences with a BaF_2 detector were measured. This detector (Scionix model 25.4 B 20/2Q-BAF-X-NEG + VD29-124KT) consists of a 20 mm thick, 25.4 mm diameter crystal mounted on an XP2020Q photomultiplier tube and has a timing resolution for 511 keV photons of about 180 ps. The LYSO and BaF_2 signals were sent to the Acqiris digitizer.

3. Results and discussion

For the measurements with picosecond laser pulses, only MPPC traces containing a single pulse and no afterpulses are used for further analysis. The fraction of pulses that are distorted by afterpulses and spontaneous breakdowns increases with increasing operating voltage. For the 400-microcell MPPC, the fraction of single photo-electron pulses that are distorted by afterpulses is 12% for 1.0 V over-voltage and 45% for 2.0 V over-voltage. This limits the maximum usable operating voltage (and thus also the maximum gain).

The pulse height spectrum for the 1600-microcell MPPC at low light intensity level is shown in Fig. 1. The clear peak separation demonstrates the photon counting capability of these devices and allows one to translate the peak amplitude to the number of fired cells. Because of the linear relationship between MPPC gain and reverse bias, the breakdown voltage can be determined by measuring the peak amplitude (or peak charge) as a function of operating voltage for a number of multiple-photo-electron peaks (Fig. 2).

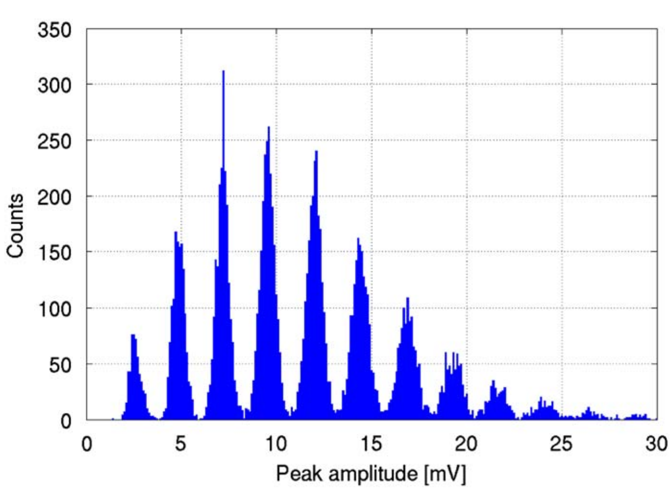

Fig. 1. Pulse height distribution for the 1600-microcell MPPC operated at 71 V. Clear separation of peaks corresponding to a different number of photo-electrons is seen.

The pulse arrival time is determined by using a digital form of constant fraction discrimination (dCFD) [8]. For each trace, the signal amplitude is determined as the difference between the signal maximum and the baseline level (Fig. 3); the latter being determined as the average of the signal samples preceding the MPPC pulse. The pulse arrival time is then taken as the time at which the rising edge of the signal crosses a trigger level equal to the baseline level plus the 30% fraction of the signal amplitude. A linear interpolation of time vs. signal between the two consecutive samples with amplitudes below and above the trigger level is performed. The arrival time of the synch out pulse is determined in the same way. However, as the synch out provides a standard pulse, its time jitter is for all practical purposes independent of the time pickoff method. A histogram of differences between the MPPC and the synch out pulse arrival times is constructed and the resulting peak fitted with a Gaussian, with the RMS timing resolution as one of the fit parameters. The timing resolution was found to be optimum for a dCFD fraction of 30%, but not very sensitive to it.

Fig. 4 shows the RMS timing resolution for the 400-microcell MPPC as a function of the number of detected photo-electrons and

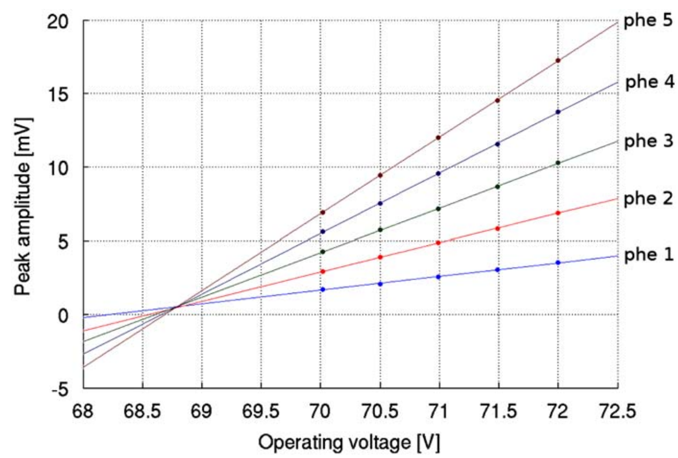

Fig. 2. Determination of the breakdown voltage for the 1600-microcell MPPC. The peak amplitudes for the 1st to the 5th photo-electron peaks are linear with operating voltage and cross at the breakdown voltage.

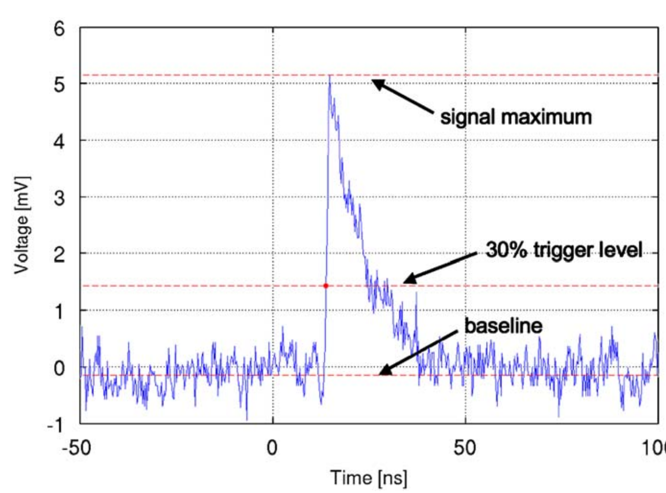

Fig. 3. Time pickoff procedure on a single photo-electron signal.

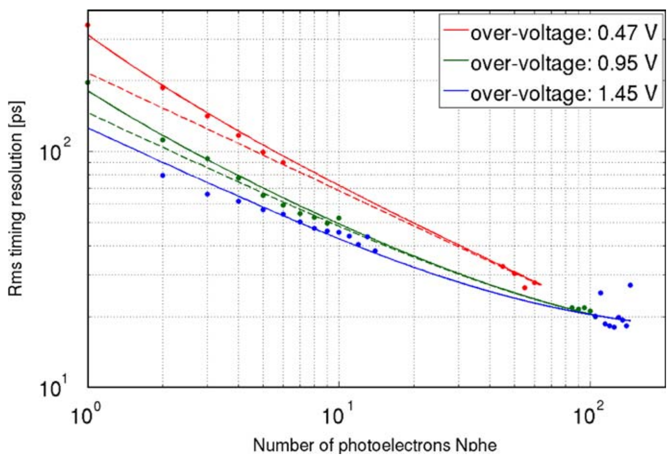

Fig. 4. RMS timing resolution as a function of the number of photo-electrons for the 400-microcell MPPC for several operating voltages (voltage above breakdown is indicated). Solid lines represent the fit of Eq. (2). Dotted lines show the fit neglecting the electronic noise contribution and using only data points for which $N_{phe}>5$. The higher the gain (i.e. over-voltage), the smaller the difference between these fits.

for a number of operating voltages. The three contributions to the timing resolution are described below. A single-point comparison time pickoff method gives a timing error (σ_n) associated with the RMS electronic noise voltage ($\tilde{v}_n$) [9]:

$$\sigma_n = \tilde{v}_n (dv_r/dt)^{-1} \tag{1}$$

where dv_r/dt is the signal slope at the trigger point. Assuming a pulse rise time independent of pulse amplitude, the signal slope is proportional to the pulse amplitude. The amplitude scales with the MPPC gain, whereas in our measurements $\tilde{v}_n$ is constant at about 0.3 mV: σ_n thus decreases with increasing gain. As the pulse amplitude is proportional to the number of detected photo-electrons (N_{phe}), $\sigma_n \propto 1/N_{phe}$. For the data point in Fig. 4 with over-voltage 0.47 V and $N_{phe}=1$, $dv_r/dt = 1.1$ mV/ns, giving $\sigma_n = 270$ ps; the fit with Eq. (2) gives a compatible value of 230 ps. The time from when a photon enters the MPPC until the output pulse appears shows a certain jitter. This internal timing resolution of the device (σ_i) is best described by Poisson statistics, i.e. $\sigma_i \propto 1/\sqrt{N_{phe}}$. A residual contribution (σ_0) is caused by additional sources that do not depend on N_{phe}, such as sampling clock jitter and laser synch out jitter. The independent contributions add in quadrature to give the measured timing resolution (σ_m):

$$\sigma_m^2 = \sigma_i^2 + \sigma_n^2 + \sigma_0^2 = \frac{\sigma_{i,spe}^2}{N_{phe}} + \frac{\sigma_{n,spe}^2}{N_{phe}^2} + \sigma_0^2 \tag{2}$$

where the subscript "*spe*" refers to the single photo-electron value of the corresponding RMS timing resolution. Fig. 5 shows the RMS *spe* internal timing resolution as a function of over-voltage for the MPPC devices; a *spe* timing resolution down to about 100 ps is obtained.

In the measurements with the LYSO crystal, the highest scintillation photon flux on the photosensor occurs during the initial moments of the scintillation process. The associated time spread is therefore lowest when triggering on the first detected photon [10]. The fastest photons are those travelling in a straight line to the photosensor. Due to the geometric mismatch between the $2\times2\,\text{mm}^2$ scintillator side and the $1\times1\,\text{mm}^2$ MPPC, we estimate a 4-fold loss in the detection of these fastest photons and, according to Poisson statistics, a 2-fold loss in timing resolution. The low number of scintillation photons hitting the

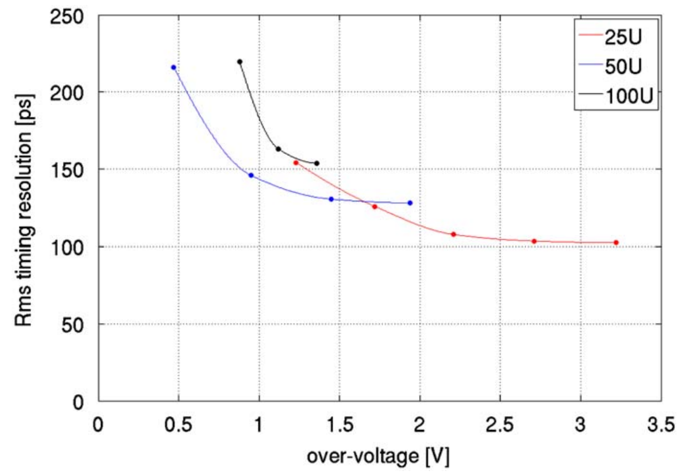

Fig. 5. RMS single photo-electron timing resolution as a function of over-voltage.

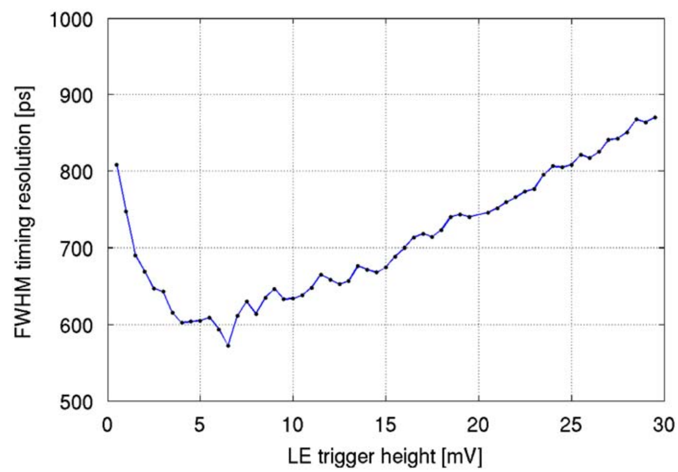

Fig. 6. FWHM coincidence timing resolution between a BaF_2 reference detector and a LYSO crystal mounted on a 100-microcell MPPC as a function of leading edge trigger level of the LYSO detector. Time pickoff on the BaF_2 is also performed by leading edge triggering.

sensor (about 400 of 13 000 for the full absorption of a 511 keV annihilation photon) points to a non-optimal intrinsic optical coupling of the crystal to the sensor; optimizing this coupling should improve the timing resolution further. Although a less than optimum timing performance is thus to be expected, we could investigate the optimum time pickoff procedure in an efficient manner by using the same set of stored digitized detector pulses. Events for which the full 511 keV photon energy was detected in both detectors were selected for analysis.

Our results confirm that it is best to trigger on the first photon detected. Fig. 6 shows the best timing resolution using a leading edge trigger at a trigger level for the LYSO detector equivalent to 1–1.5 photo-electrons, about 3% of the 511 keV signal height. For trigger levels comparable to the noise level, the timing performance decreases as the trigger level crossing time is influenced by the noise. In these measurements, the combination of digitizer quantization noise and preamplifier electronic noise was 1.5 mV RMS; an increase in timing resolution is observed for trigger levels <4 mV.

The best timing resolution was obtained for the 100-microcell MPPC because it has a higher photon detection efficiency (PDE) due to its higher fill factor, resulting in a higher fraction of detected initial scintillation photons.

References

[1] J.S. Karp, S. Surti, M.E. Daube-Witherspoon, G. Muehllehner, J. Nucl. Med. 49 (2008) 462.
[2] W.W. Moses, IEEE Trans. Nucl. Sci. NS-50 (2003) 1325.
[3] T.K. Lewellen, Semin. Nucl. Med. 28 (1998) 268.
[4] An overview of the most recent developments can be found in these proceedings and e.g. in the Proceedings of the IEEE NSS/MIC Conferences ⟨www.nss-mic.org⟩.
[5] G. Collazuol, et al., Nucl. Instr. and Meth. A 581 (2007) 461.
[6] M.S. Judenhofer, H.F. Wehrl, D.F. Newport, et al., Nat. Med. 14 (2008) 459.
[7] M.C. Maas, D.J. van der Laan, D.R. Schaart, J. Huizenga, J.C. Brouwer, P. Bruyndonckx, S. Léonard, C. Lemaitre, C.W.E. van Eijk, IEEE Trans. Nucl. Sci. NS-53 (2006) 1071.
[8] L. Bardelli, G. Poggi, M. Bini, G. Pasquali, N. Taccetti, Nucl. Instr. and Meth. A 521 (2004) 480.
[9] T.H. Wilmshurst, Signal Recovery from Noise in Electronic Instrumentation, Hilger, London, 1985.
[10] R.F. Post, L.I. Schiff, Phys. Rev. 80 (1950) 1113.